Ni@rGO Nanocomposites as Heterogenous Catalysts for Thiocarboxylation Cross-Coupling Reactions

Lorenzo Lombardi,[a] Raffaello Mazzaro,[b,c] Massimo Gazzano,[d] Alessandro Kovtun,[d] Vittorio Morandi,[b,c] Giulio Bertuzzi[a] and Marco Bandini[a,e]*

[a] Dipartimento di Chimica "Giacomo Ciamician", Alma Mater Studiorum – Università di Bologna, via Selmi 2, Bologna, Italy [+39-051-2099751, marco.bandini@unibo.it]

[b] CNR-IMM, Via Piero Gobetti 101, 40129 Bologna, Italy.

[c] Dipartimento di Fisica e Astronomia "A. Righi", Alma Mater Studiorum – Università di Bologna, via Berti Pichat 6/2, Bologna, Italy.

[d] Istituto per la Sintesi Organica e Fotoreattività (ISOF) – CNR, via Gobetti 101, 40129 Bologna.

[e] Consorzio CINMPIS, Università di Bologna, via Selmi 2, Bologna, Italy.

Table of Contents

SEM/TEM characterization

Nanoscale characterization of the materials was performed by Scanning and Transmission electron microscopy techniques (SEM and TEM). SEM analysis was performed on a Zeiss Leo 1530 FE-SEM operated at 5 kV. TEM analysis was carried out with a FEI Tecnai F20 Shottky-FEG HR-TEM operated at 120kV, equipped with EDAX X-Rays EDS spectrometer and Fischione STEM-HAADF detector. The samples were dispersed in isopropanol and drop casted on Quantifoil Cu R1/2 carbon coated TEM grids.

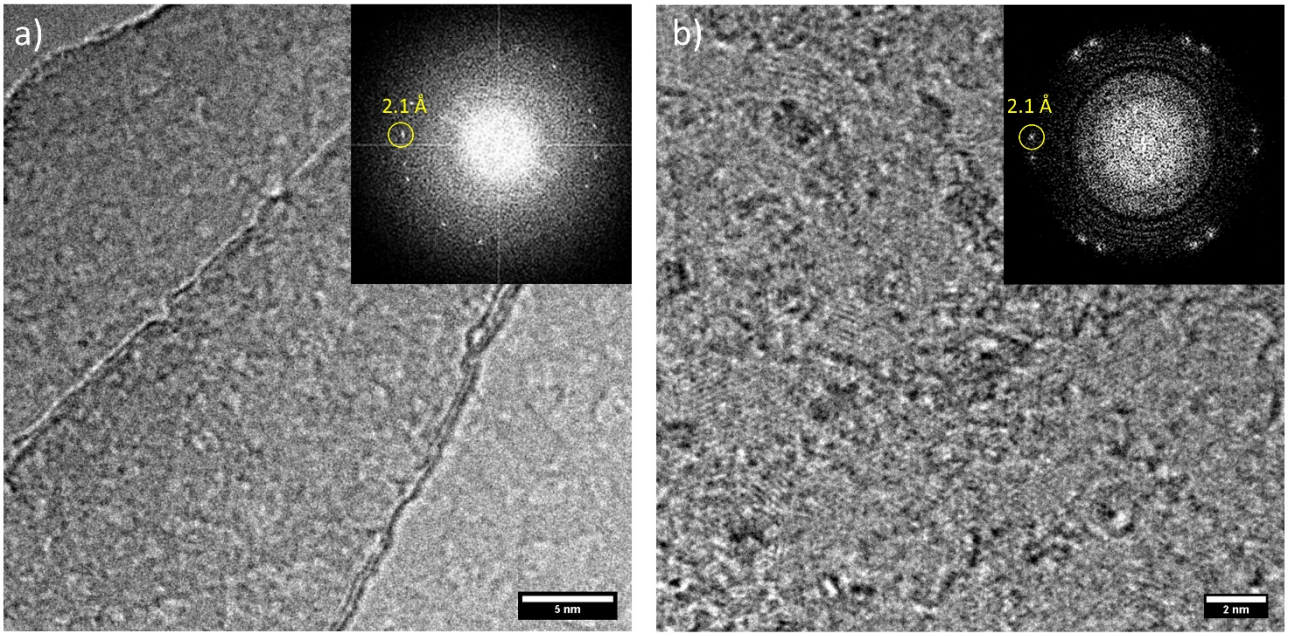

Figure S1. High magnification HR-TEM micrographs of the rGO supporting material in a) **NiNP@rGO Type 1** and b) **NiNP@rGO Type 2**. In the inset, the Fast Fourier Transformate exhibiting 2.1 Å-spaced diffraction fringes, assigned to Graphite (1,1,1) lattice planes.

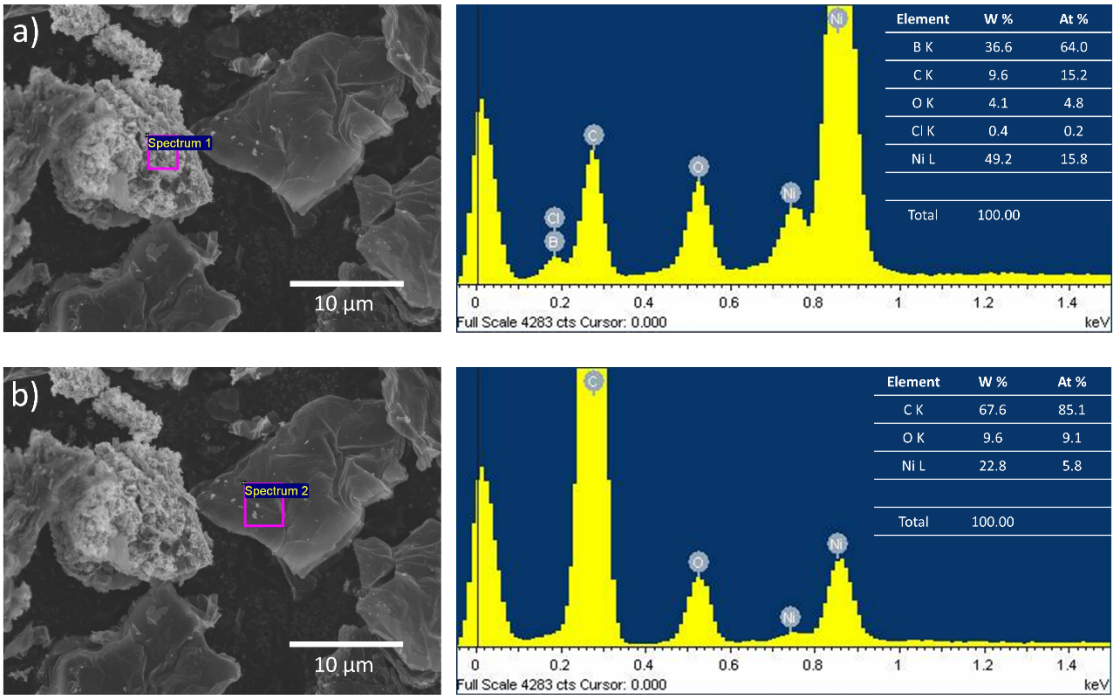

Figure S2. SEM-EDS characterization of different micro-aggregates on sample **NiNP@rGO Type 2**, displaying different composition (table in the inset) rising from the presence of a) Nickel Boride contamination and b) NiNPs decorated rGO flakes.

X-Ray Photoelectron Spectroscopy characterization

XPS spectra were acquired by hemispherical analyser (Phoibos 100, Specs, Germany) by using a Mg Kα excitation. Survey and high-resolution spectra were acquired in Fixed Analyser transmission (FAT) mode, with energy resolution 0.9 eV measured on freshly sputtered Silver (Ag 3d). Spectrometer was calibrated to Au $4f_{7/2}$ peak at 84.0 eV. The solid dry powders was deposited on conductive Carbon tape and degassed overnight. Charging effects was corrected by calibrating all spectra to C 1s 284.6 eV. Deconvolutions were performed by using CasaXPS software after Shirley background subtraction. C1 was fitted by using asymmetric line-shape for aromatic Carbon and symmetric line-shapes (pseudo-voigt) for the C-O defects.[4a] The O/C ratio was obtained from C 1s fit according the stoichiometric ratios of C-O groups. Ni 2p was fitted by using asymmetric line-shape (LA(1.1,2.2,10) line-shape in CasaXPS) for metallic Ni(0) and pseudo voigt for Ni(II) and shake-up transitions.[4b] The reference for binding energy for Ni was taken from ref. 4c.[4c]
After the chemical reduction the typical contaminants of GO, as S and Cl were removed. The amount of Nitrogen (N 1s) increases in **Type 1,** due to the hydrazine residuals.

Sample	C 1s 284.6eV	O 1s 532eV	N 402eV	S 2p 168.4eV	Cl 2p 199.4eV	Ni 2p (II) 856.3eV	Ni 2p(0) 852.8eV
GO	69.0	27.8	0.9	1.2 ± 0.3	0.8 ± 0.2	-	-
NiNP@rGO Type 1	85.0	12.2	1.5	-	-	0.23 ± 0.05	-
NiNP@rGO Type 2	68.8	24.5	-	-	-	4.7 ± 0.3	2.0± 0.3

Table S1. Chemical composition (atomic %) of the surface obtained by XPS survey of GO, **NiNP@rGO Type 1** and **NiNP@rGO Type 2**. Binding energy (eV) was reported for each transition. Errors are typically: ±0.8 % for values higher that 25%; ±0.3 % for values between 25 % and 3 %.

Sample	C=C sp^2	C-C sp^3	C-OH	C-O-C	C=O	O-C=O	O/C
GO	39.9	7.3	15.9	29.2	5.4	2.3	0.41 ± 0.01
Ni@NP-rGO Type 1	79.4	7.3	7.9	2.1	3.0	0.3	0.13 ± 0.01
Ni@NP-rGO Type 2	52.7	21.3	15.2	6.7	3.8	0.3	0.23 ± 0.01

Table S2. C 1s deconvolution of GO, **NiNP@rGO Type 1** and **NiNP@rGO Type 2**. Values in % of the total C 1s signal.

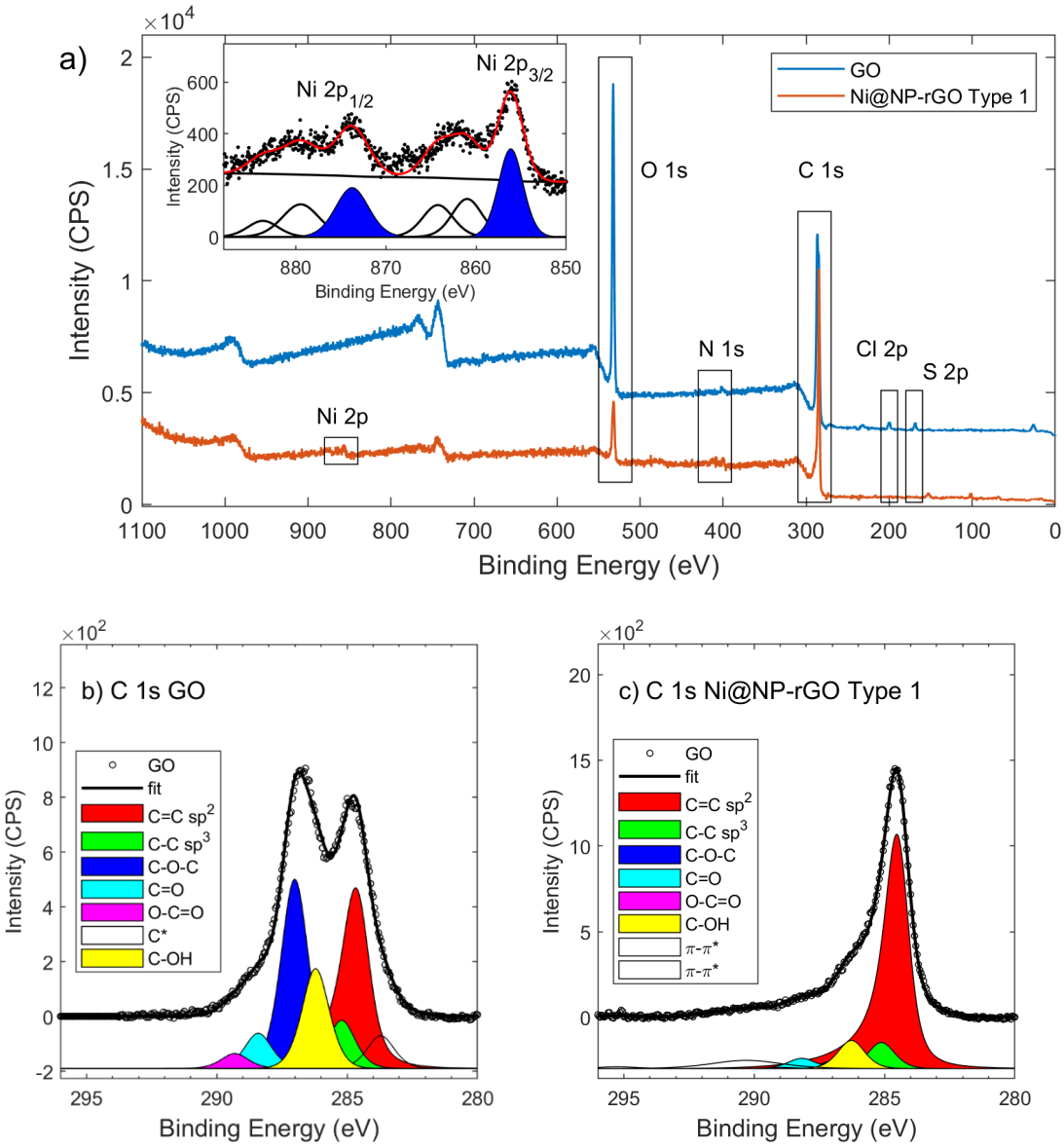

Figure S3. a) XPS survey spectra of GO and **NiNP@rGO Type 1**, inset Ni 2p signal fitted with doublet in blue and shake-up transition. b) C 1s signal of pristine GO. c) C 1s signal of **NiNP@rGO Type 1**.

Table S3. Additional optimization data

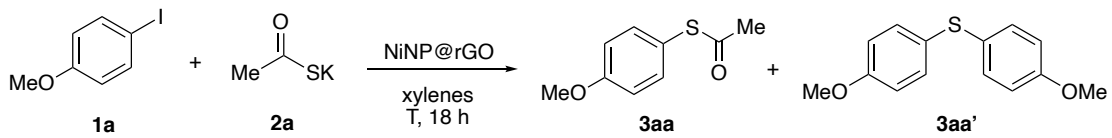

Entry[a]	Temperature	1a : 2a	NiNPs@rGO loading	Yield (%)[b]	3aa : 3aa'[c]
1	150	1 : 6	8 mg	60[d]	> 25 : 1
2	120	1 : 6	8 mg	25	> 25 : 1
3	130	1 : 6	8 mg	42	> 25 : 1
5	150	1 : 8	8 mg	70[d]	> 25 : 1
6	150	1 : 3	8 mg	65	3.7 : 1
7	150	1 : 12	8 mg	65	15 : 1
8	150	1 : 6	4 mg	18	> 25 : 1
9	150	1 : 6	12 mg	69	8 : 1

[a)] All the reactions were carried out under nitrogen and degassed solvent. [**1a**]: 0.2 M. [b)] ^{1}H-NMR conversion [c)] Determined by ^{1}H-NMR analysis. [d)] Isolated yield.

By running the reaction at lower temperatures (entries 2,3 compared to entry 1) lower yields were observed, confirming the need for higher temperatures (*i.e.* 150 °C). Varying the amounts of **2a** (entries 6,7 compared to entry 5) has little effect on the conversion, but it worsens the selectivity (**3aa** : **3aa'**). Lowering the amount of catalyst (entry 8 compared to entry 1) lowers the conversion significantly, while increasing the amount above the optimal 8 mg (entry 9) has no beneficial effect and slightly worsens the selectivity.

“Hot filtration” leaching experiment

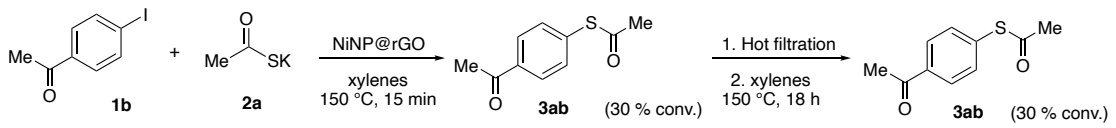

Substrate **1b** was subjected to the optimized reaction conditions according to general procedure. After 15 minutes, the reaction mixture was filtered immediately, while still hot, on a cotton plug and the filtrate was collected in a pre-flame dried Schlenk tube under nitrogen. A small portion of the mixture was withdrawn and analyzed by ^{1}H-NMR spectroscopy to assess the initial conversion of the reaction, while the rest of the mixture was sealed again and subjected to heating at 150°C for 18 h. After heating, the solvent was evaporated and a second portion was again analyzed by ^{1}H-NMR spectroscopy to assess the conversion. The second portion crude ^{1}H-NMR spectrum was identical to the one of the first portion, suggesting that: the catalyst is genuinely heterogeneous, no leaching of any active form of catalyst from the material occurs during the reaction course, and also that no appreciable reactivity of starting material or product is occurring in the absence of the catalyst.

XRD analysis of the recovered material and dried reaction mixture

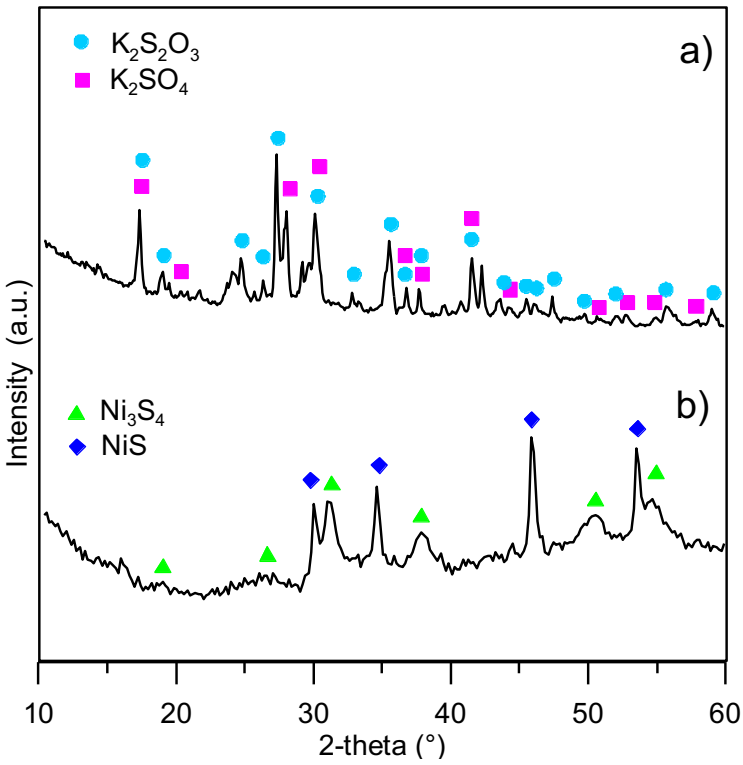

Figure S4: XRD analysis, a) of the filtered, dried mixture reaction; b) of the recovered **NiNP@rGO Type 2** catalyst after reaction. The main peaks are allocated to the reported crystalline phases. Reference files from: $K_2S_2O_3$ ICDD 01-0694, K_2SO_4 ICDD 25-0681, Ni_3S_4 ICSD:60-1828, NiS COD 9009240 (ICDD International Centre for Diffraction)

Copy of ^{1}H, ^{13}C and ^{19}F NMR Spectra

3aa ^{1}H NMR (400 MHz, $CDCl_3$)

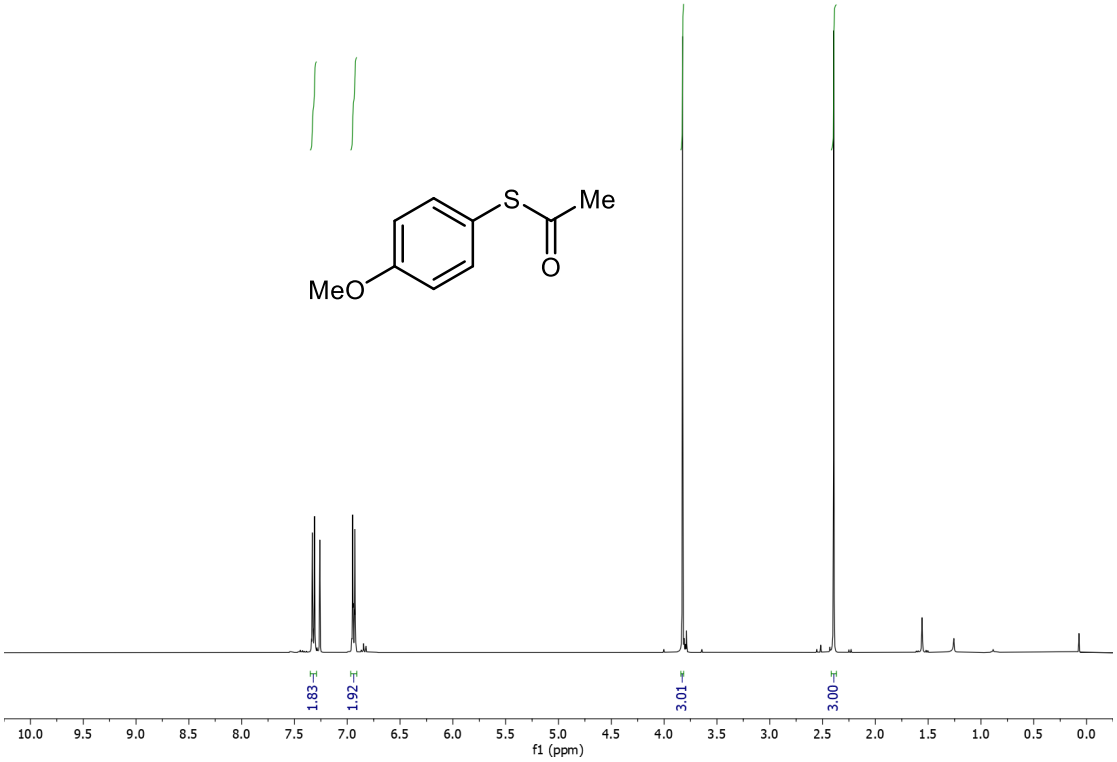

3aa ^{13}C NMR (100 MHz, $CDCl_3$)

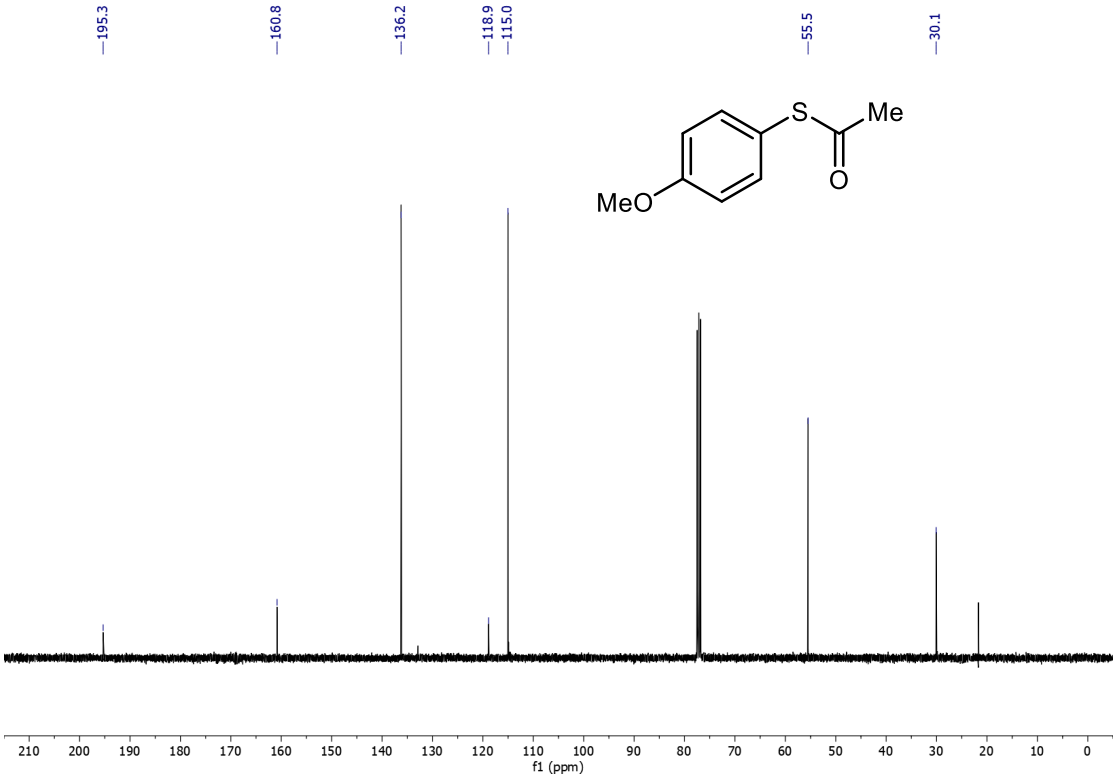

3ba ^{1}H NMR (400 MHz, $CDCl_3$)

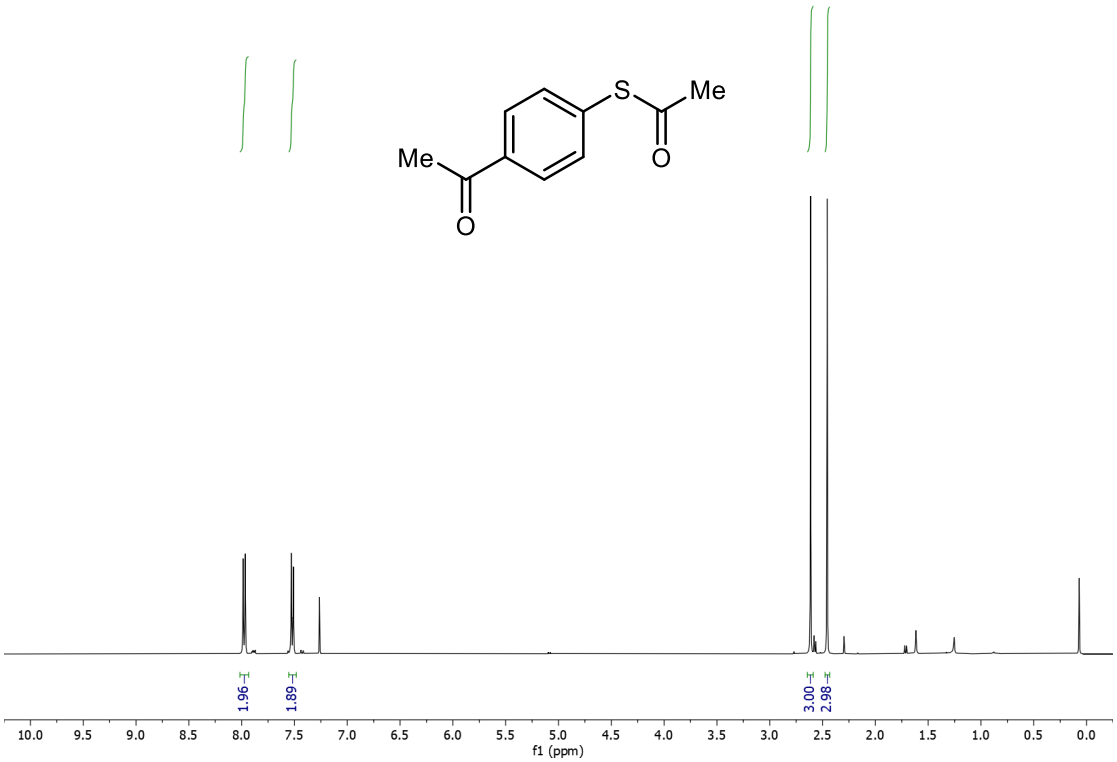

3ba ^{13}C NMR (100 MHz, $CDCl_3$)

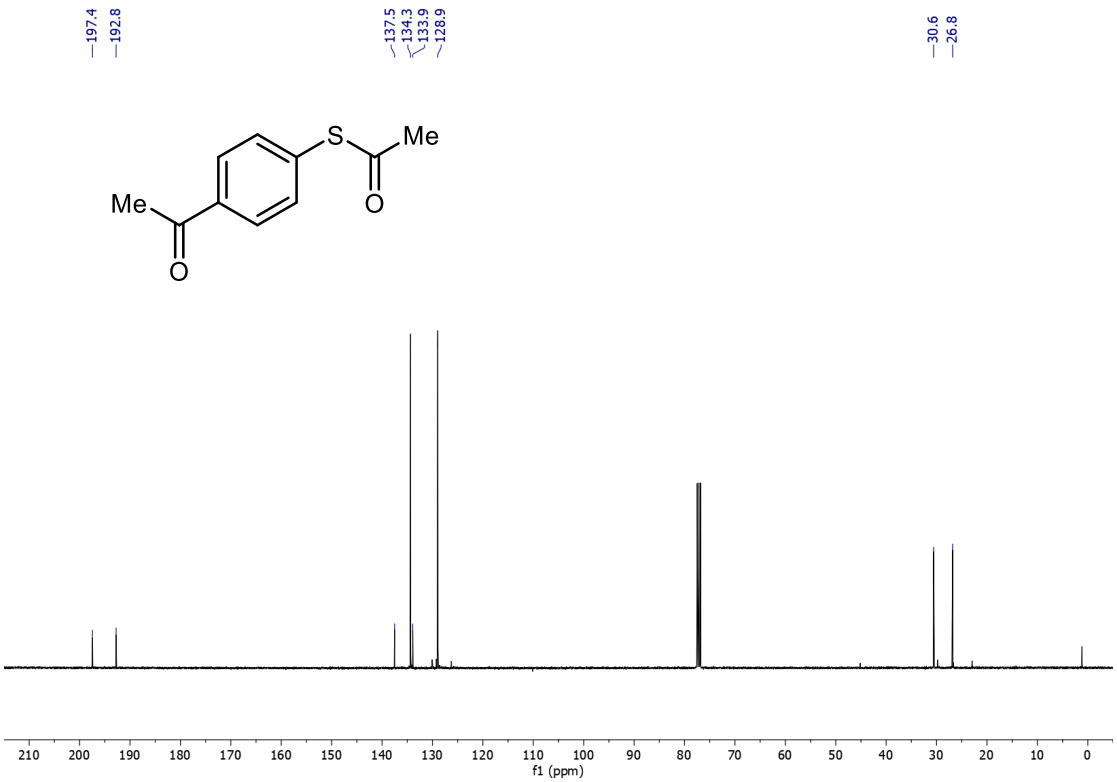

3ca ^{1}H NMR (400 MHz, $CDCl_3$)

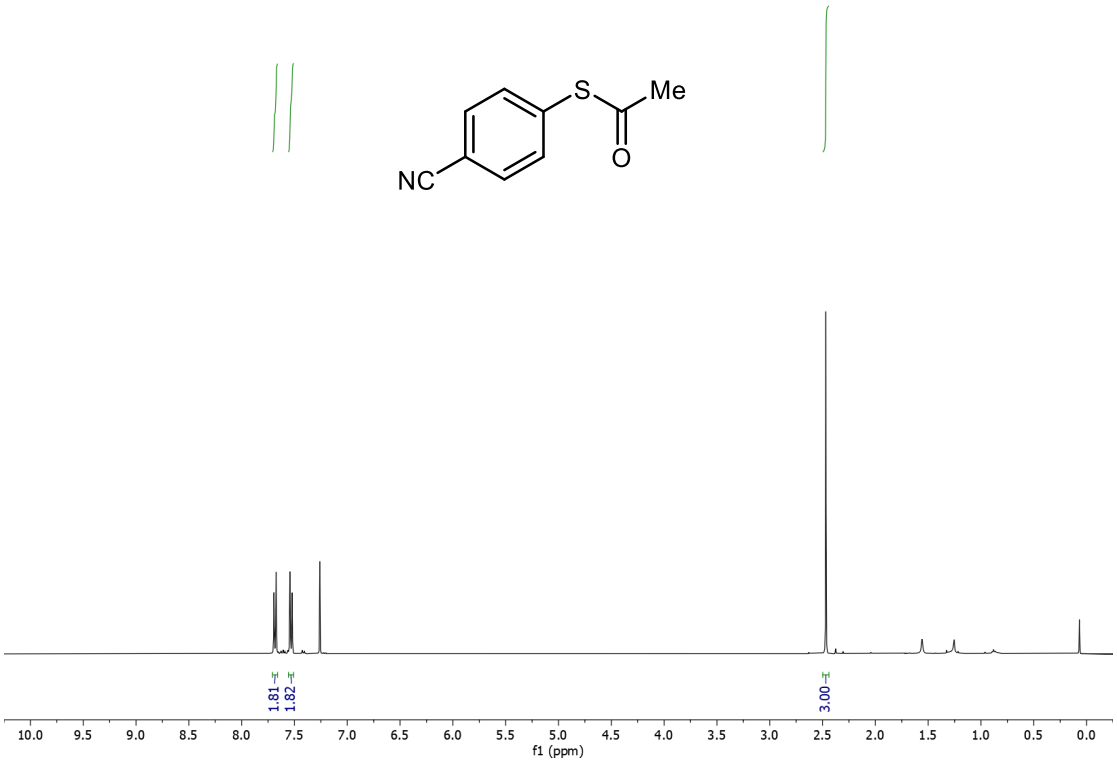

3ca ^{13}C NMR (100 MHz, $CDCl_3$)

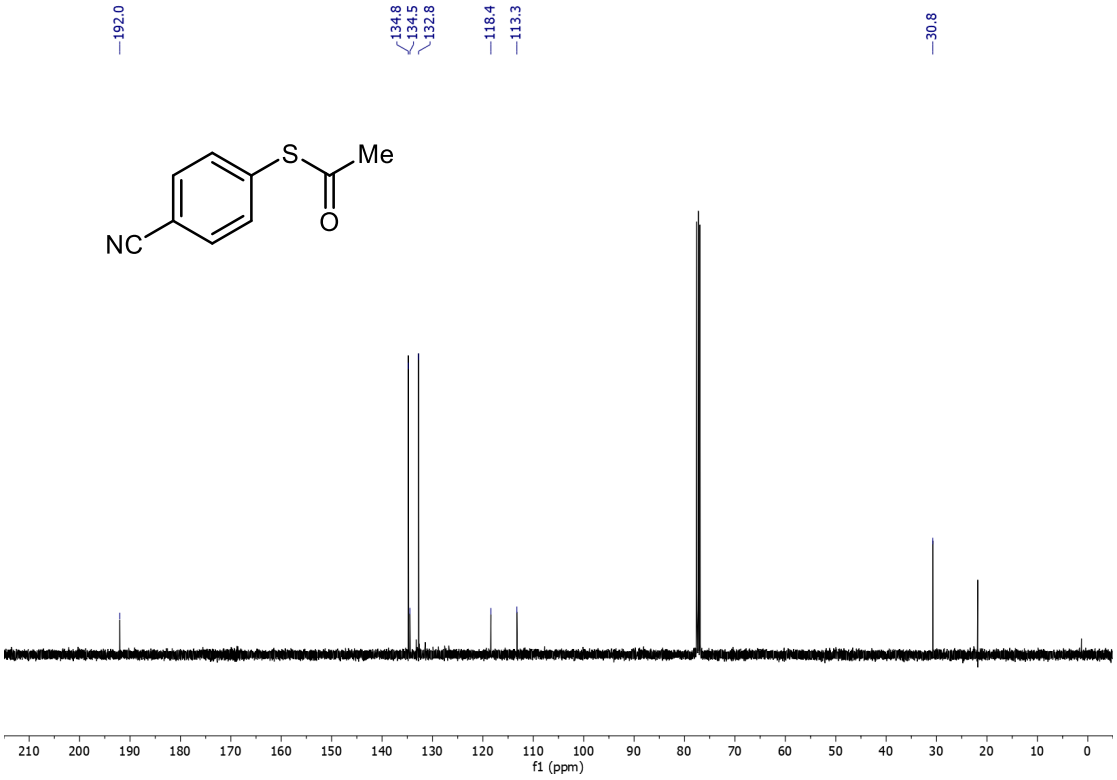

3da ^{1}H NMR (400 MHz, $CDCl_3$)

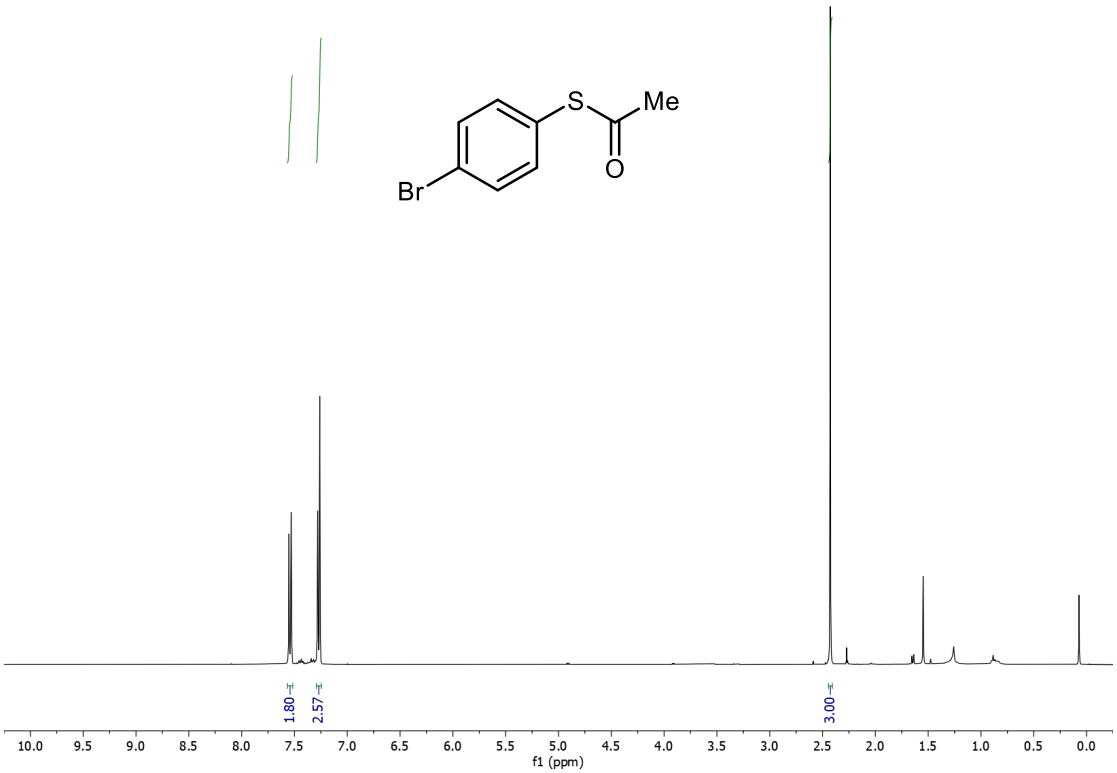

3da ^{13}C NMR (100 MHz, $CDCl_3$)

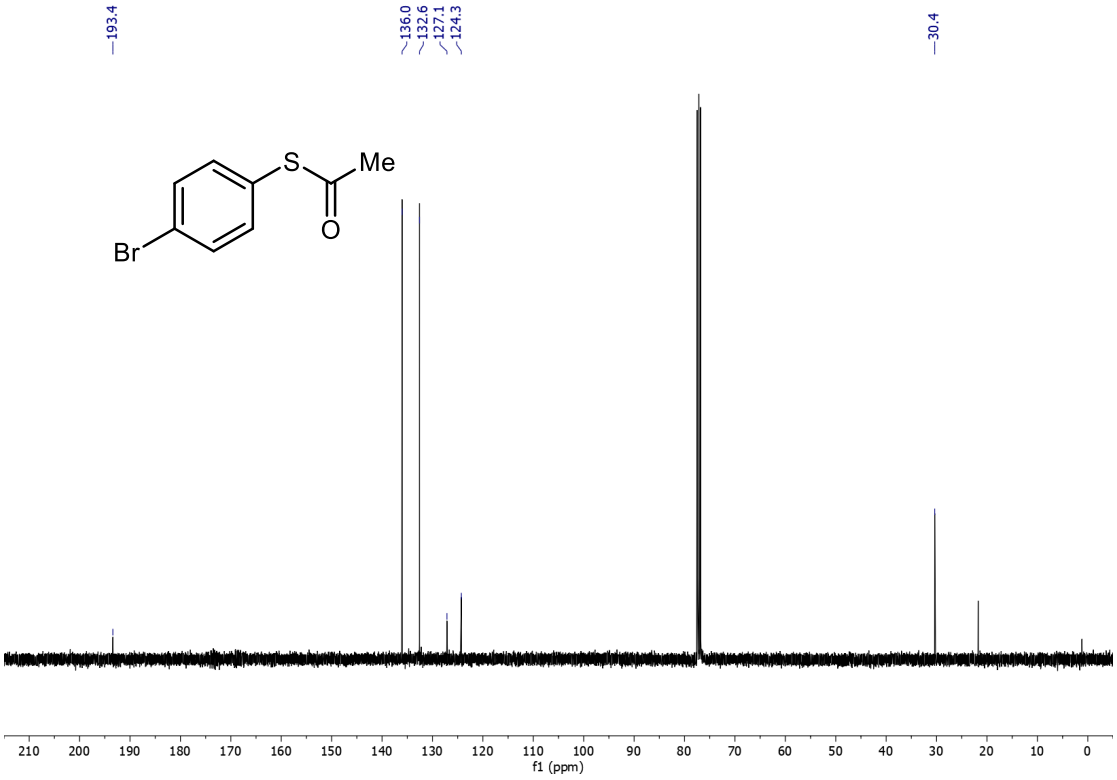

3ea ^{1}H NMR (400 MHz, $CDCl_3$)

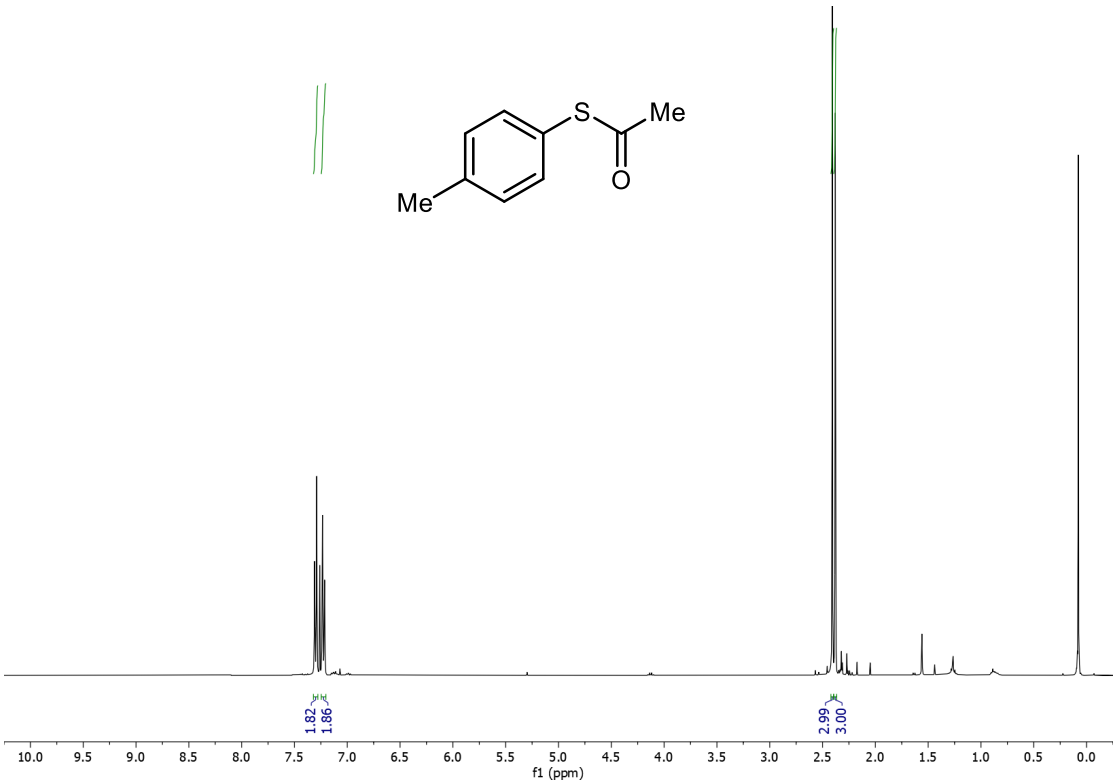

3ea ^{13}C NMR (100 MHz, $CDCl_3$)

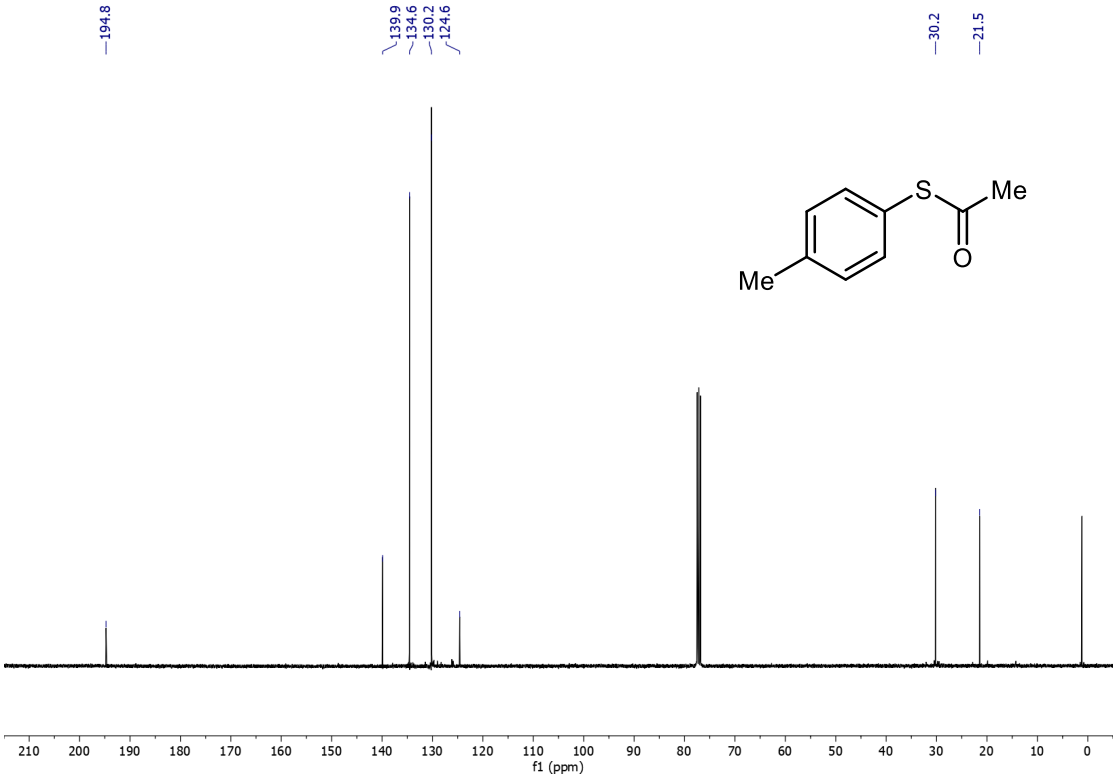

3fa ^{1}H NMR (400 MHz, $CDCl_3$)

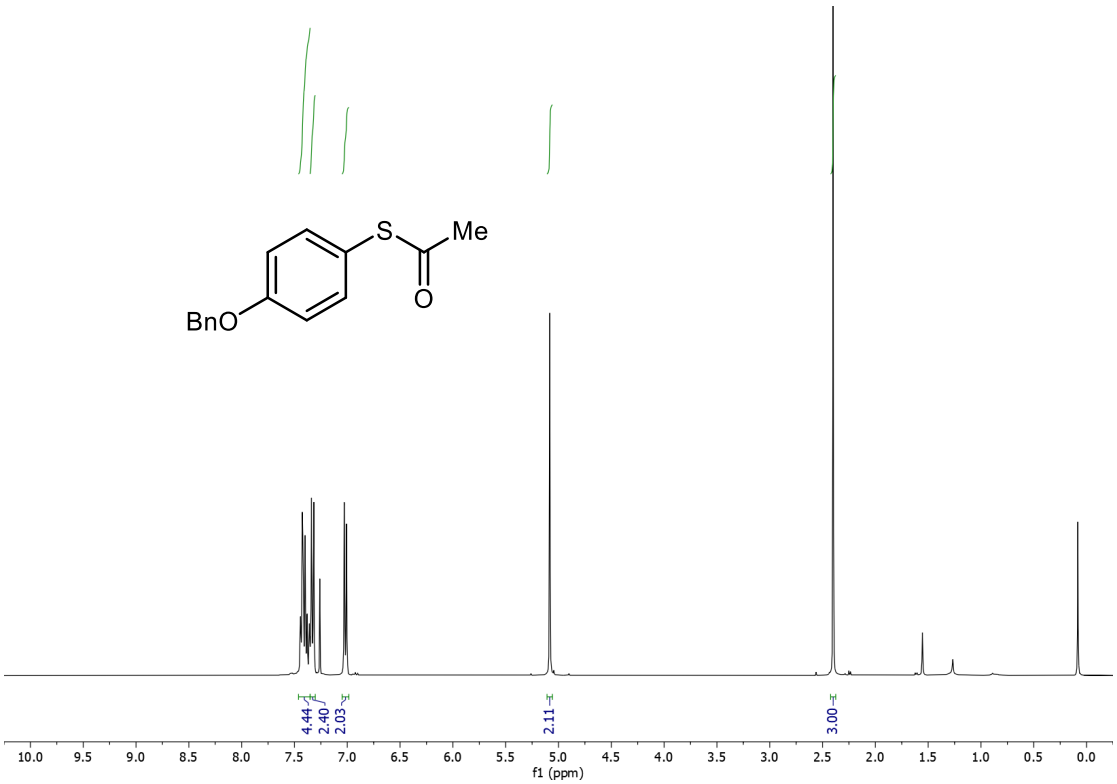

3fa ^{13}C NMR (100 MHz, $CDCl_3$)

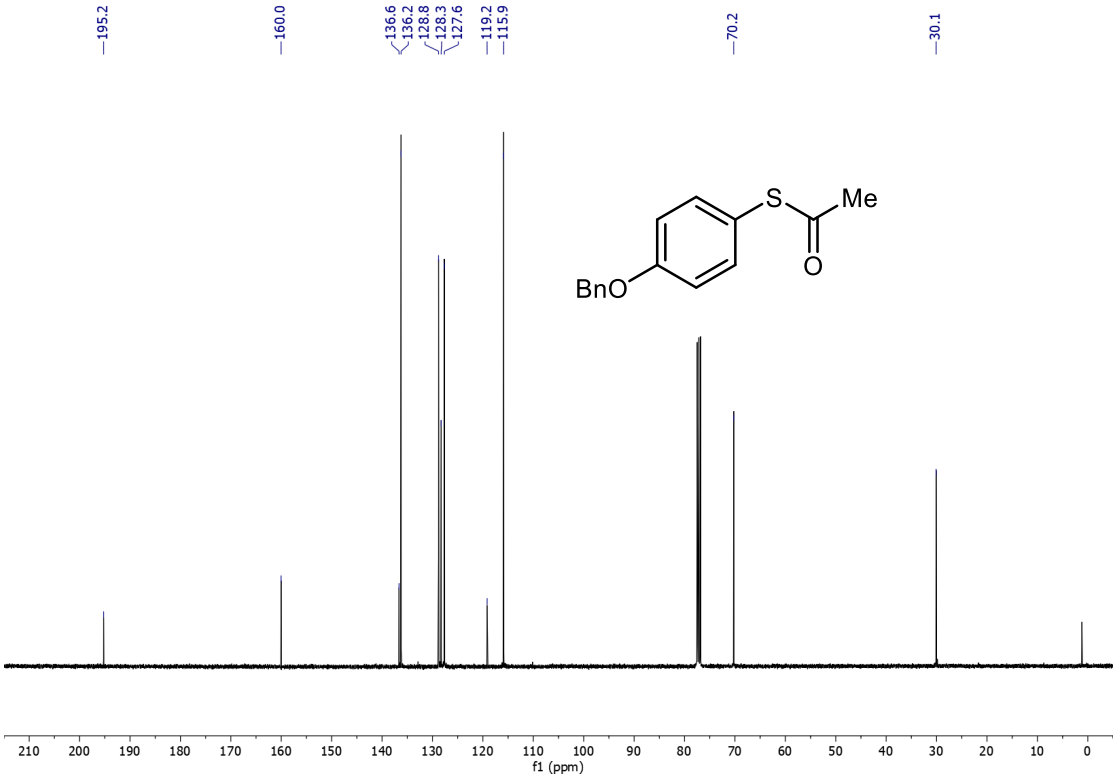

3ga ^{1}H NMR (400 MHz, $CDCl_3$)

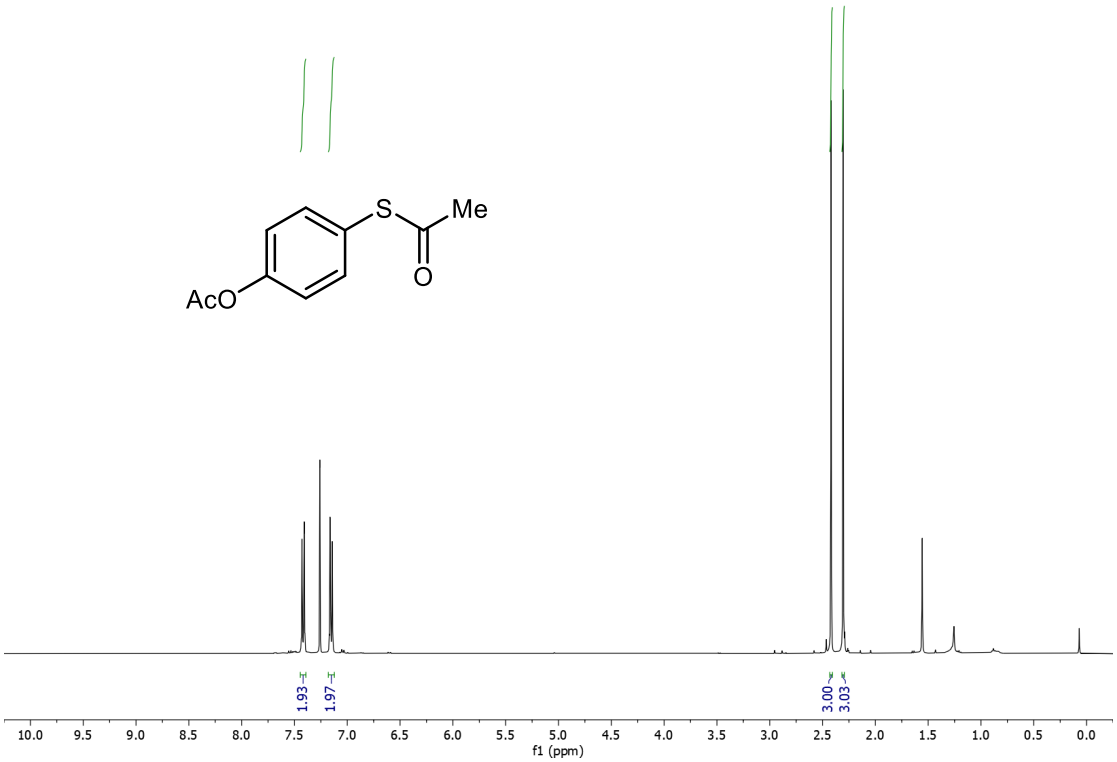

3ga ^{13}C NMR (100 MHz, $CDCl_3$)

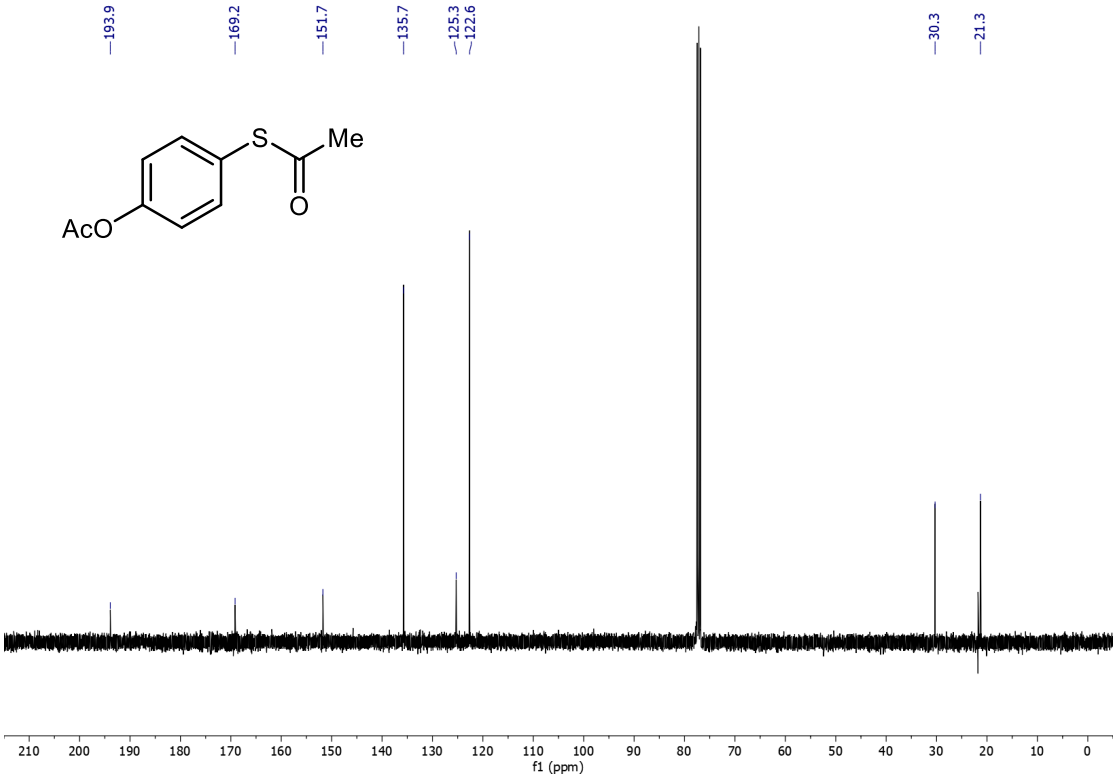

3ha ^{1}H NMR (400 MHz, $CDCl_3$)

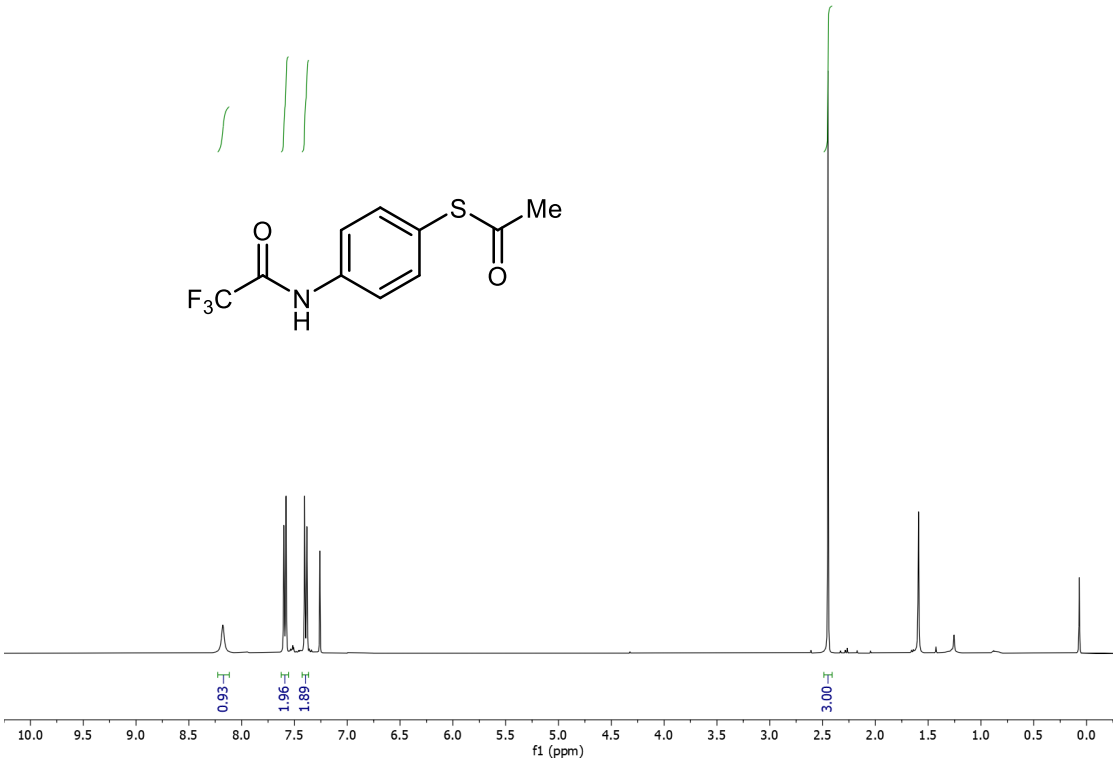

3ha ^{13}C NMR (100 MHz, $CDCl_3$)

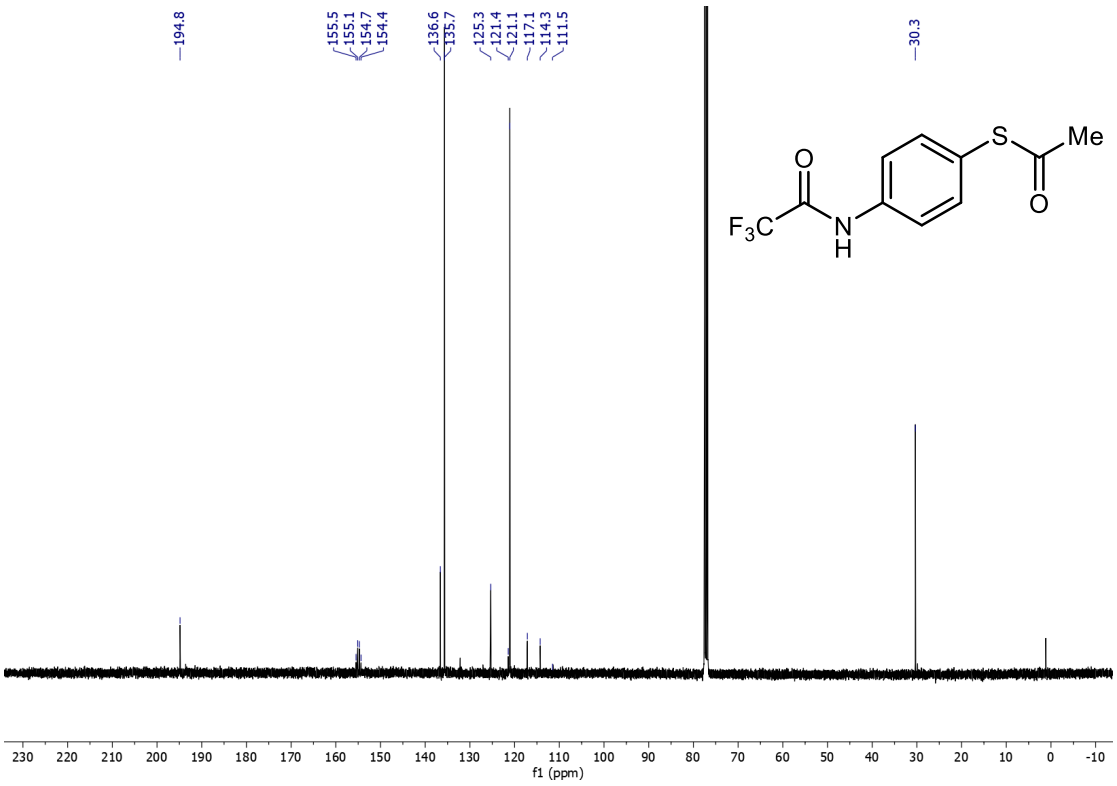

3ha ^{19}F NMR (376 MHz, $CDCl_3$)

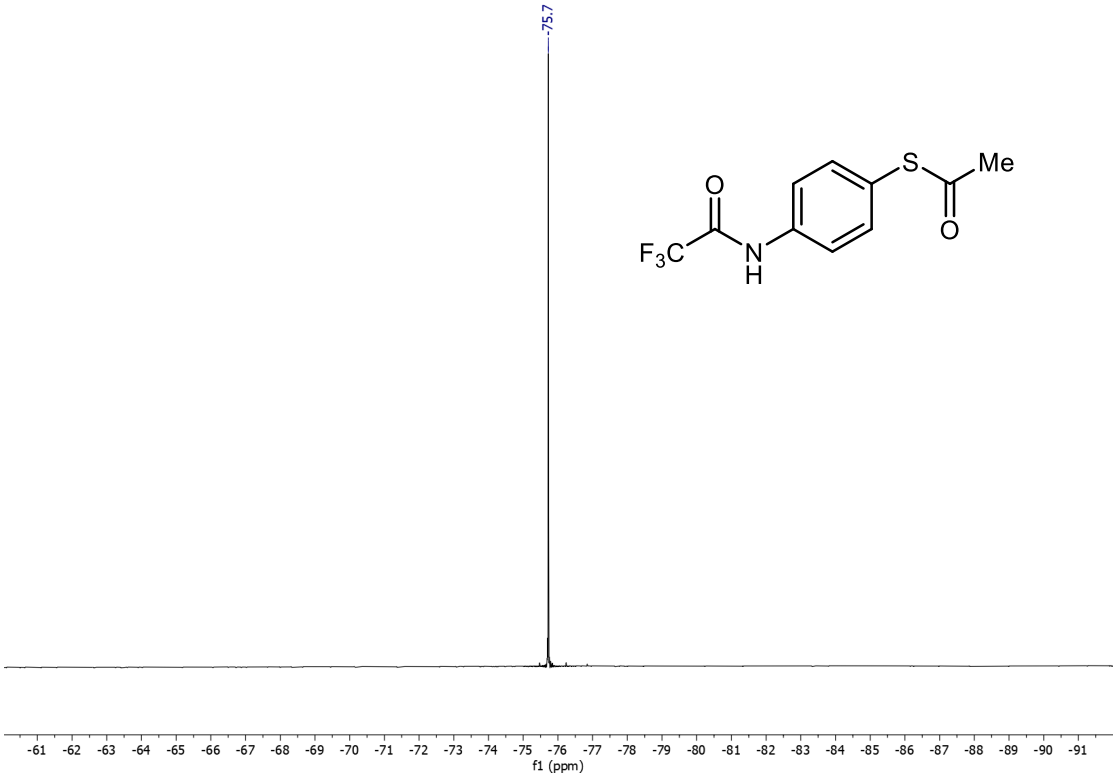

3ia ^{1}H NMR (400 MHz, $CDCl_3$)

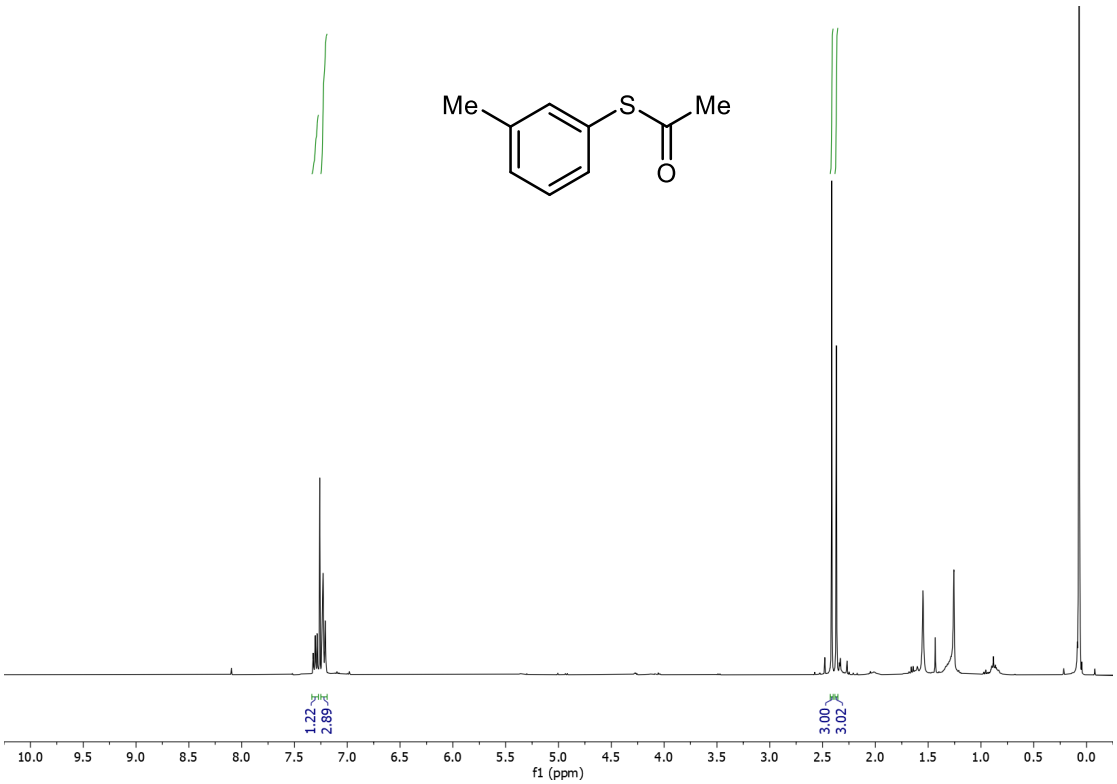

3ia ^{13}C NMR (100 MHz, $CDCl_3$)

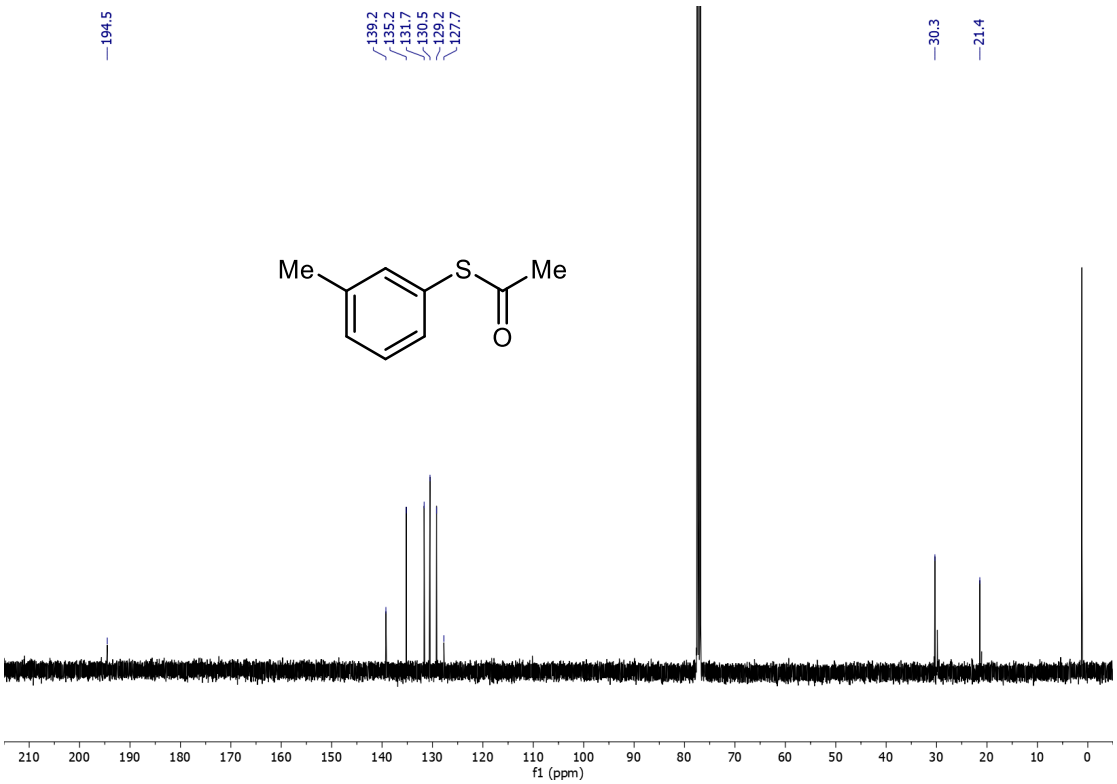

3ja ^{1}H NMR (400 MHz, $CDCl_3$)

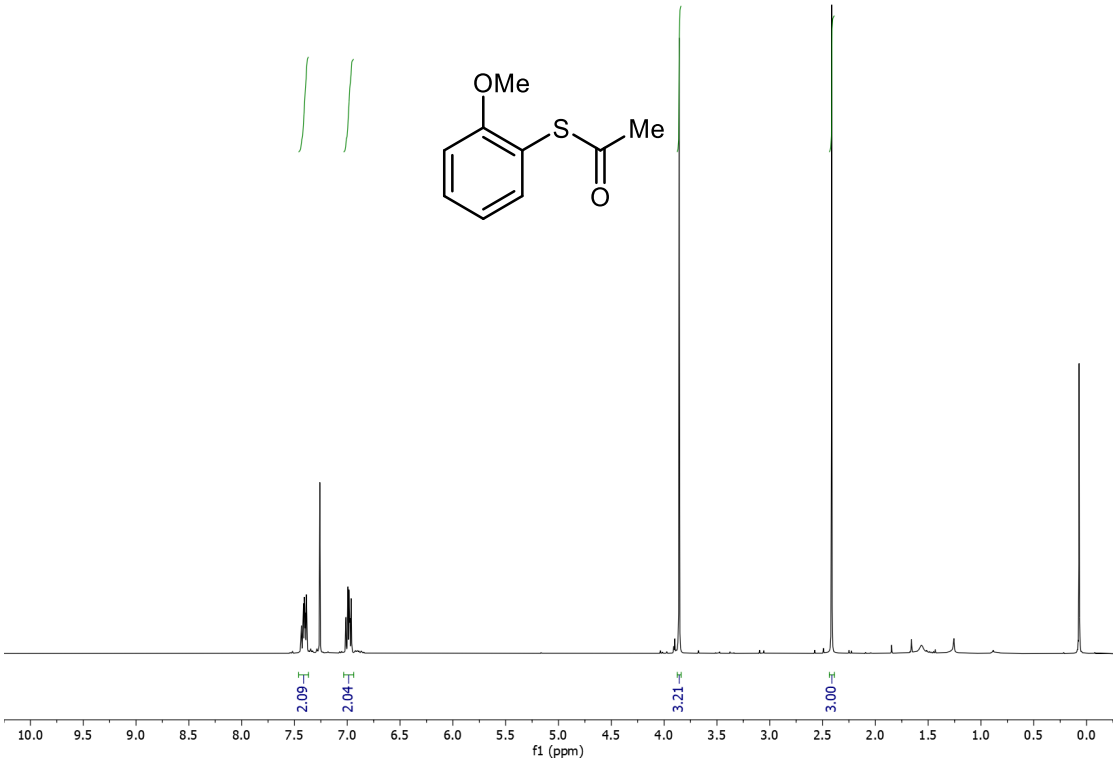

3ja ^{13}C NMR (100 MHz, $CDCl_3$)

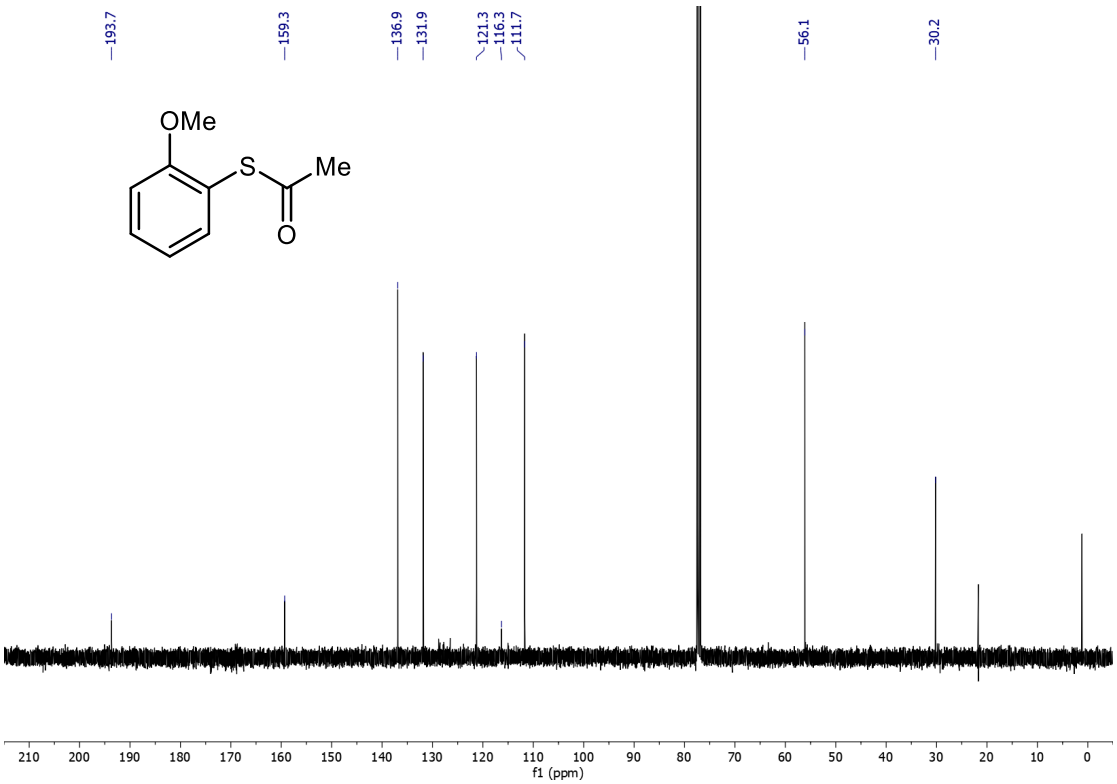

3ka ^{1}H NMR (400 MHz, $CDCl_3$)

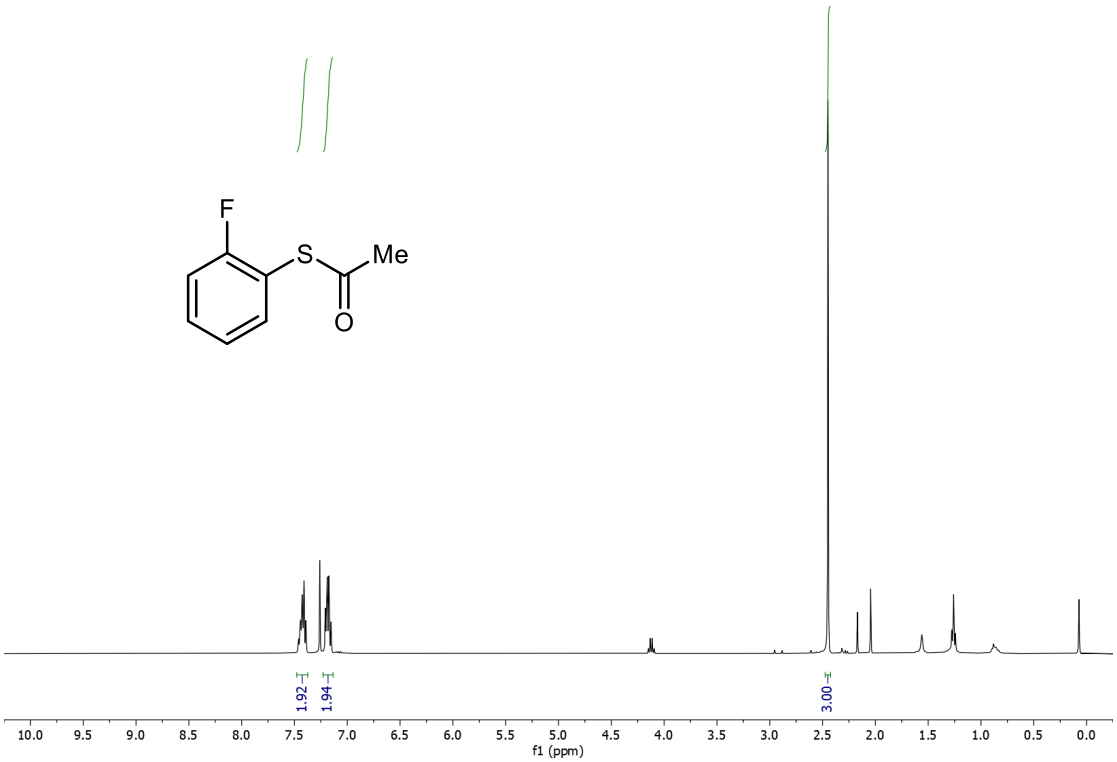

3ka ^{13}C NMR (100 MHz, $CDCl_3$)

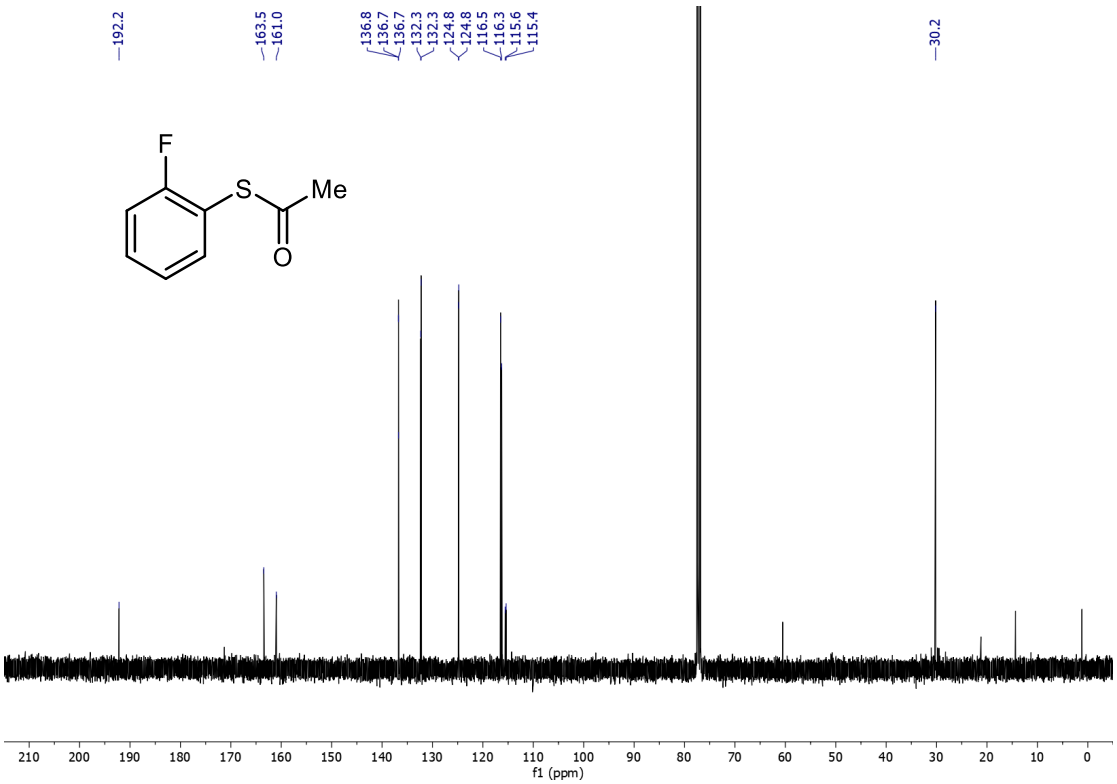

3ka ^{19}F NMR (376 MHz, $CDCl_3$)

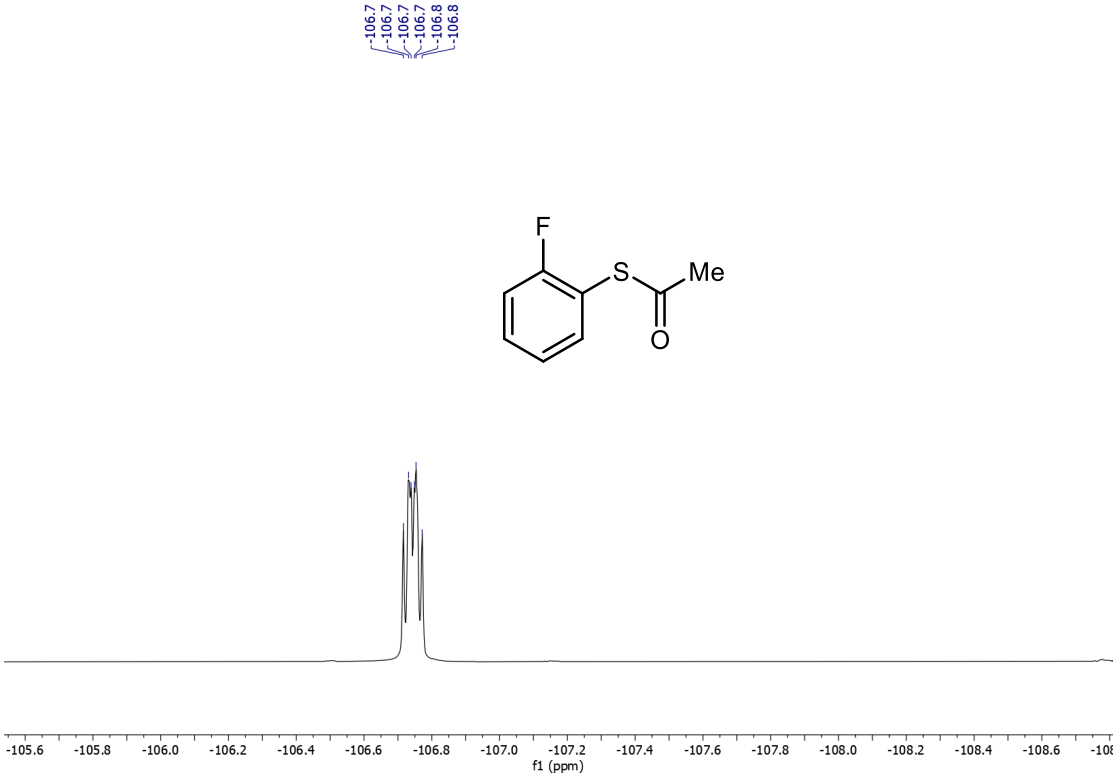

3la ^{1}H NMR (400 MHz, $CDCl_3$)

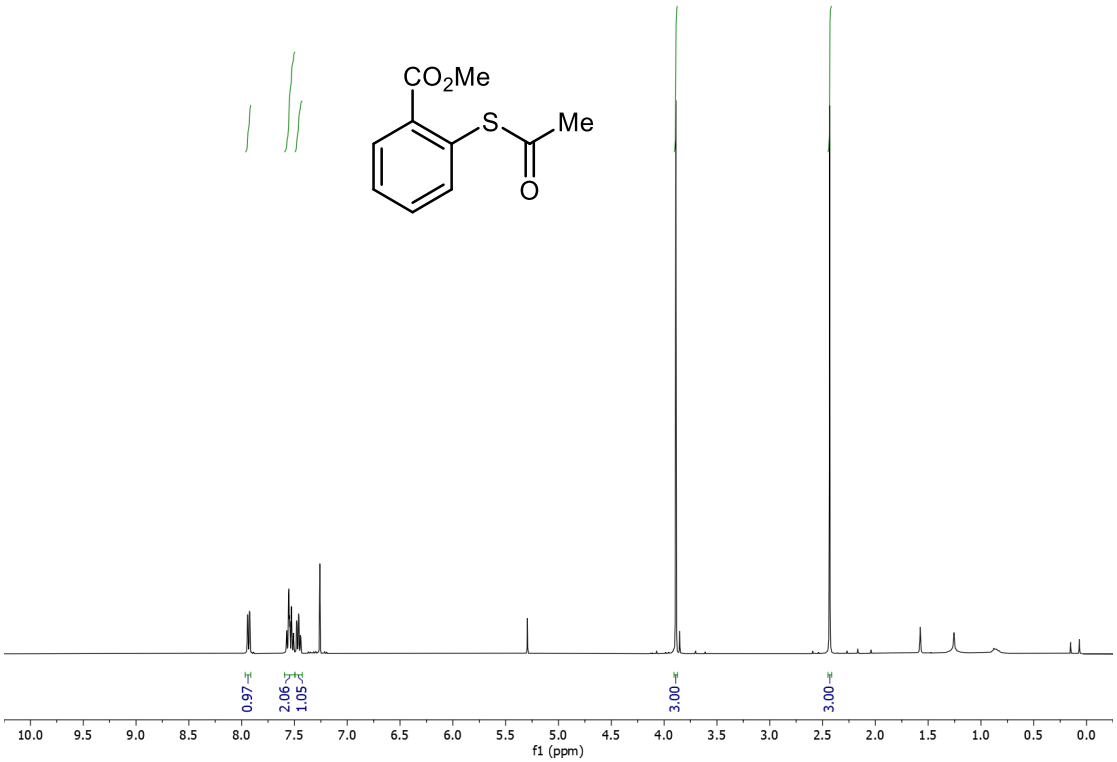

3la ^{13}C NMR (100 MHz, $CDCl_3$)

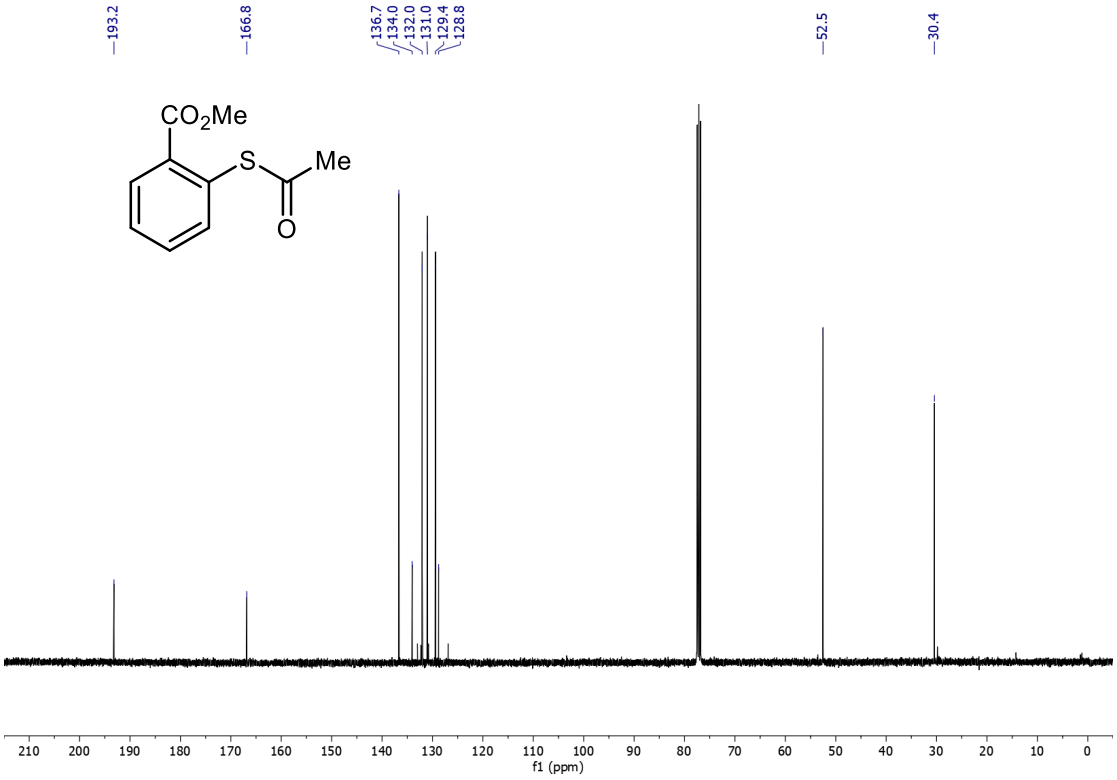

3ma ^{1}H NMR (400 MHz, $CDCl_3$)

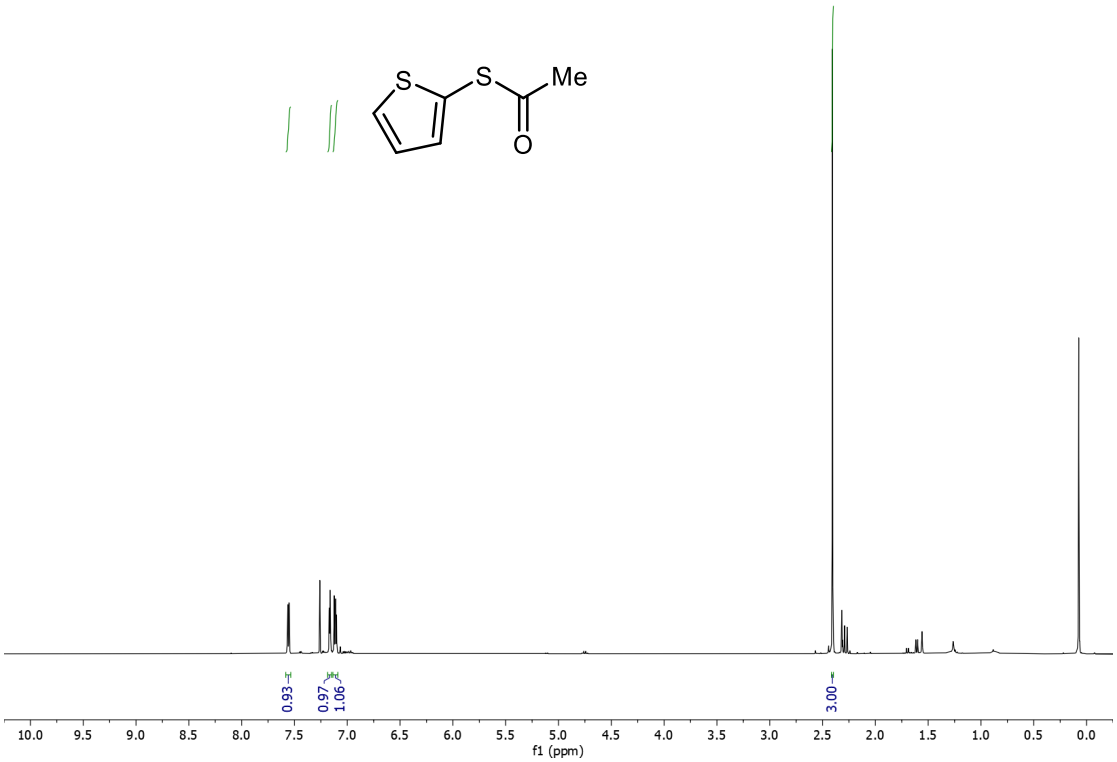

3ma ^{13}C NMR (100 MHz, $CDCl_3$)

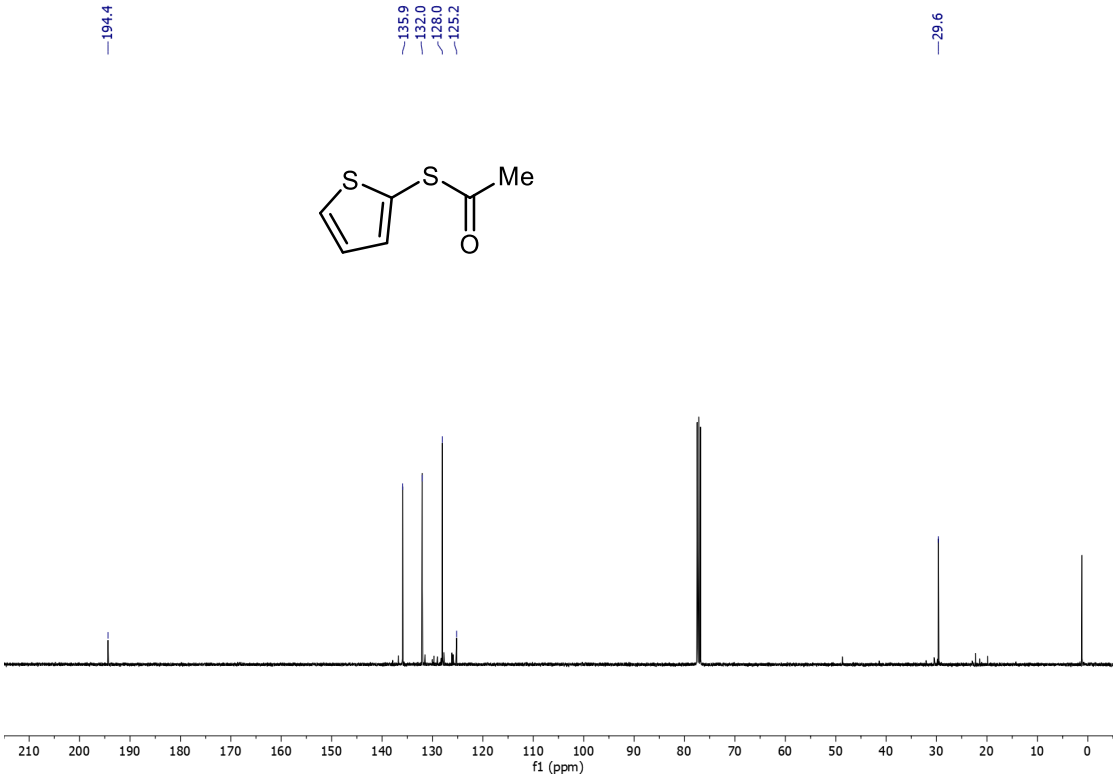

3na ^{1}H NMR (400 MHz, $CDCl_3$)

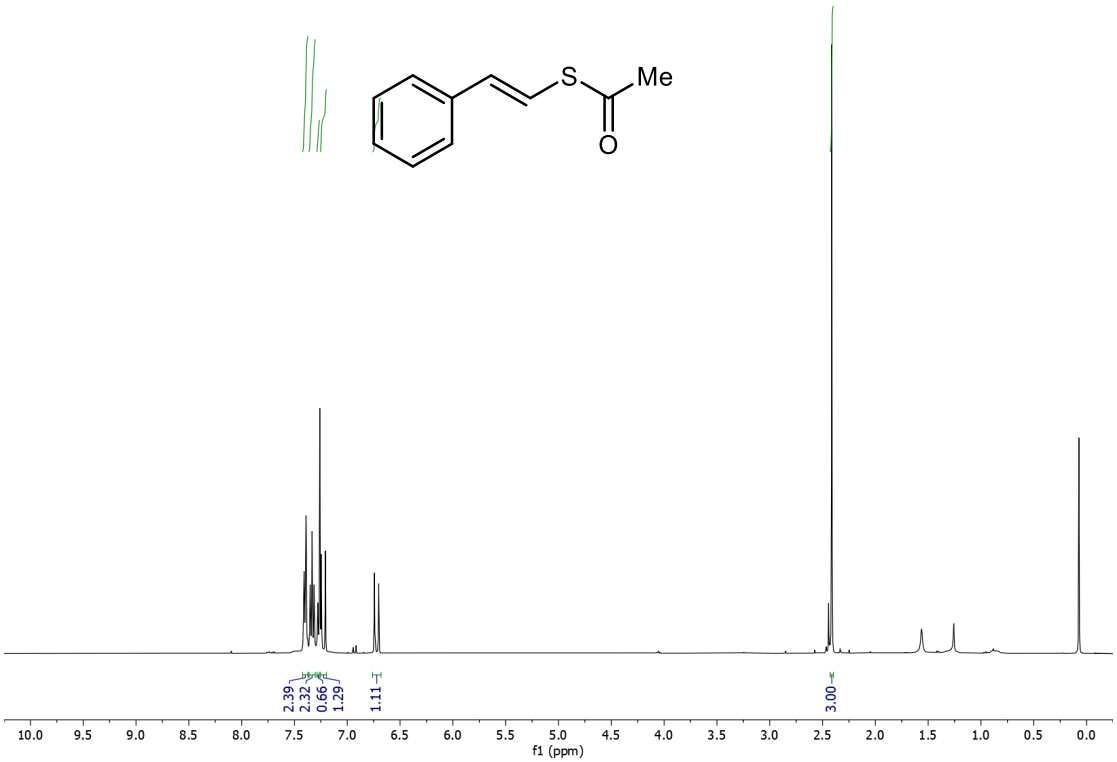

3na ^{13}C NMR (100 MHz, $CDCl_3$)

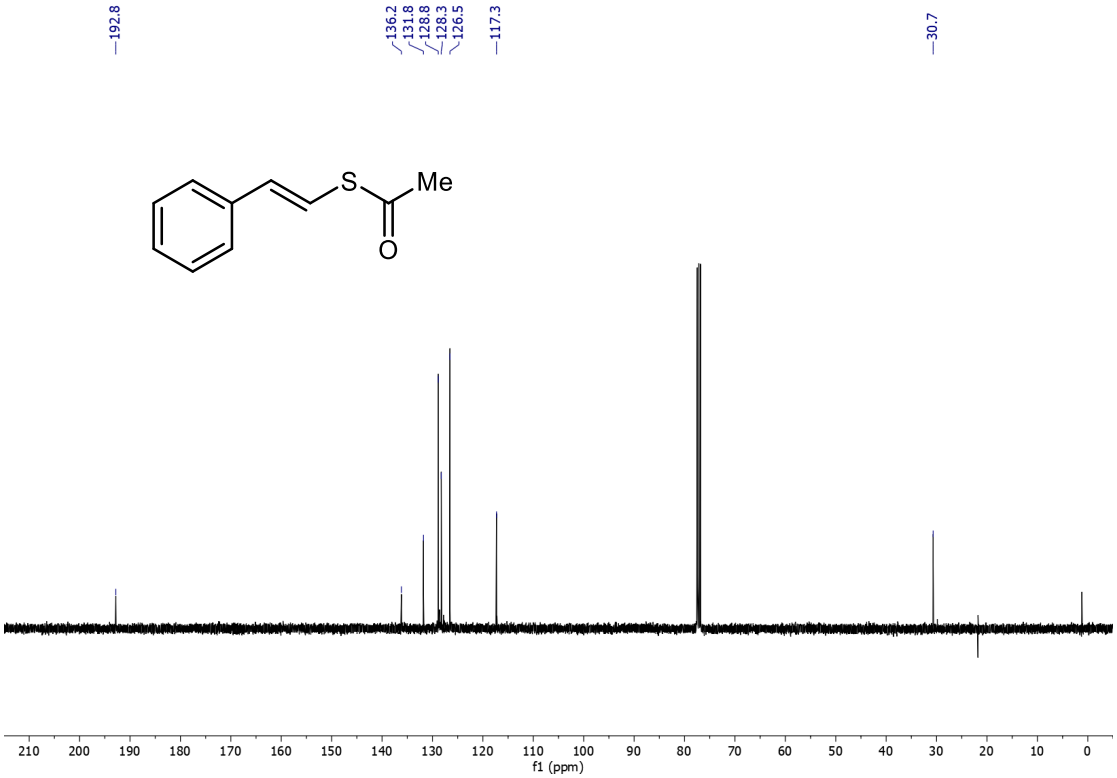

3bb ^{1}H NMR (400 MHz, $CDCl_3$)

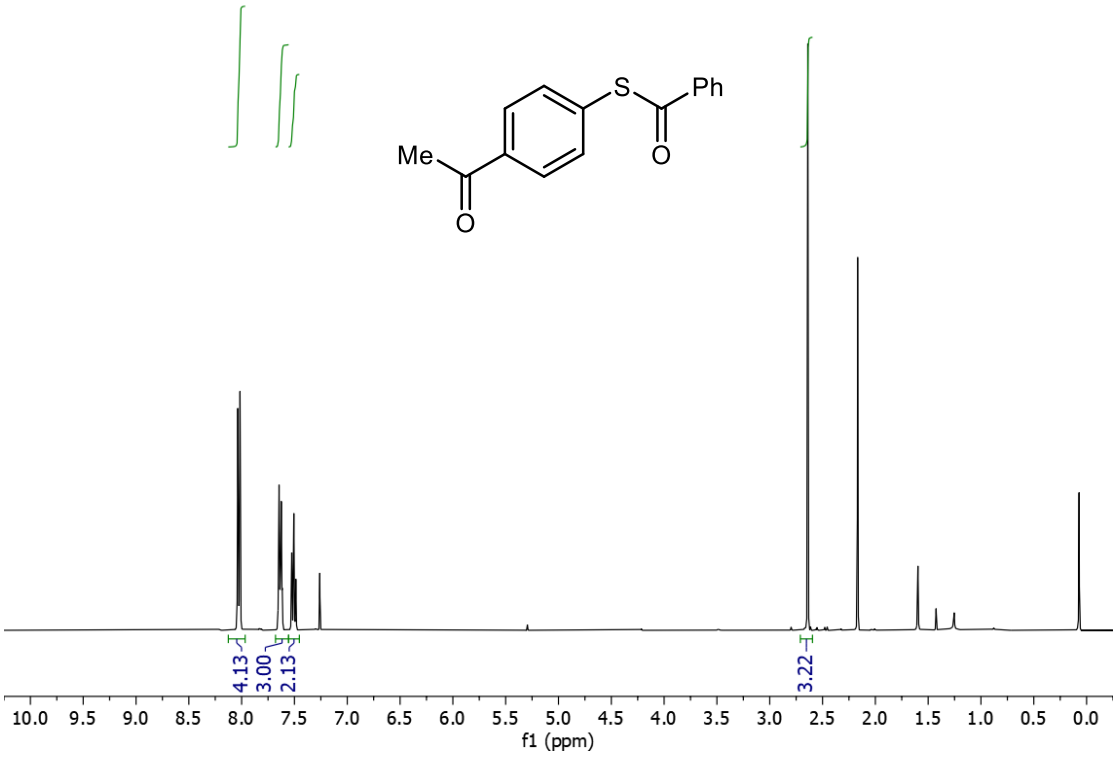

3bb ^{13}C NMR (100 MHz, $CDCl_3$)

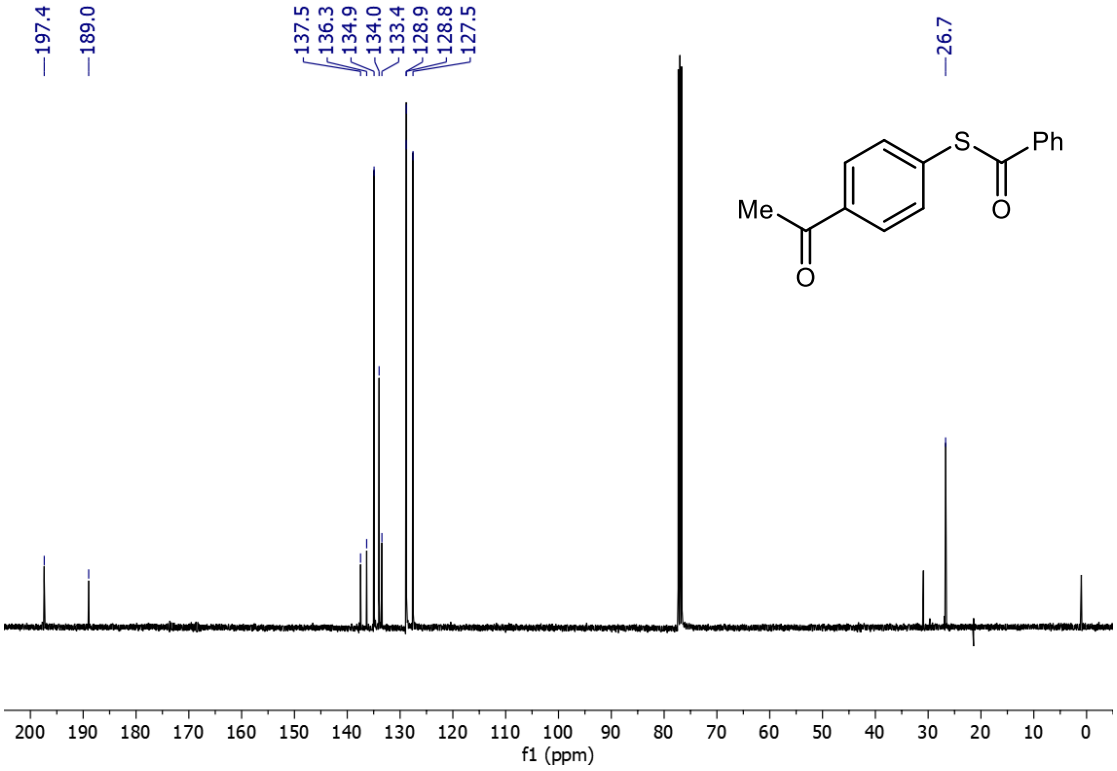

References

[1] a) A. Kovtun, D. Jones, S. Dell'Elce, E. Treossi, A. Liscio, V. Palermo, *Carbon* **2019**, *143*, 268 – 275. b) M. C. Biesinger, B. P. Payne, A. P. Grosvenor, L. W. M. Lau, A. R. Gerson, R. St. C. Smart, *Appl. Surf. Sci.* **2011**, *257*, 2717 – 2730. c) K. S. Kim, N. Winograd, *Surf. Sci.* **1974**, *43*, 625 – 643.